Assessing a Model-of-Models Approach for Global Flood Forecasting and Alerting

Bandana Kar ⬤, Guy J.-P. Schumann ⬤, Marina T. Mendoza ⬤, Doug Bausch ⬤, Jun Wang ⬤, Prativa Sharma ⬤, and Margaret T. Glasscoe ⬤

Abstract—**Flooding is a frequent extreme weather event that causes significant financial and societal losses. According to the International Disaster Database (EM-DAT), during January through July 2023, 87 flooding events caused about 2000 deaths and $13 billions in damages globally. Among the impacted, low- and medium-income countries with resource scarcity tend to experience high mortality, displacement of people, unmitigated damages, and long-term recovery. Currently, several hydrologic models and Earth observation (EO) datasets are used to forecast flood severity and impacts. However, not all of these models are globally operational or publicly available. The variability in outputs in terms of accuracy, scale, and content also limits their usage for emergency response activities. The Model of Models (MoM), an ensemble approach, integrates hydrologic models and EO datasets 1) to forecast flood risk (probability of occurrence) globally every 24 h at a subwatershed level and 2) to disseminate alert messages and potential impact information to at-risk communities using the Pacific Disaster Center's DisasterAWARE platform. MoM is operational and designed to assist countries with flood risk management and mitigation by providing early warning and situational awareness information. An accuracy assessment of MoM from user-perspective across nine different flood types revealed that 1) the model reliably generated early warning for 100% of the flooded subwatersheds in seven events, and 2) during 2022 flooding, 61% and 89% of the flooded subwatersheds that were identified to be in Watch and Warning categories in Pakistan and Chad, respectively, were detected to be flooding by the Copernicus Global Flood Monitoring system.**

Index Terms—**Early warning, Earth observation (EO) data, global flood forecasting, hydrologic models, Model of Models (MoM).**

I. INTRODUCTION

FLOODING is one of the most frequent and costly extreme weather events. According to the International Disaster Database (EM-DAT), during 2000–2022, flood-induced

Bandana Kar is with the U.S. Department of Energy, Washington, D.C. 20585 USA (e-mail: bandana.kar@ee.doe.gov).

Guy J.-P. Schumann is with ImageCat, Inc., Long Beach, CA 90802 USA, and also with the School of Geographical Sciences, University of Bristol, Bristol, U.K.

Marina T. Mendoza is with ImageCat, Inc., Long Beach, CA 90802 USA.

Doug Bausch is with Niyam IT, Leesburg, VA 20175 USA.

Jun Wang is with Indiana University, Bloomington, IN 47405 USA.

Prativa Sharma is with the Bennett & Pless, Atlanta, GA 30346 USA.

Margaret T. Glasscoe is with the University of Alabama, Tuscaloosa, AL 35899 USA, and also with NASA-Marshall Space Flight Center, Huntsville, AL USA.

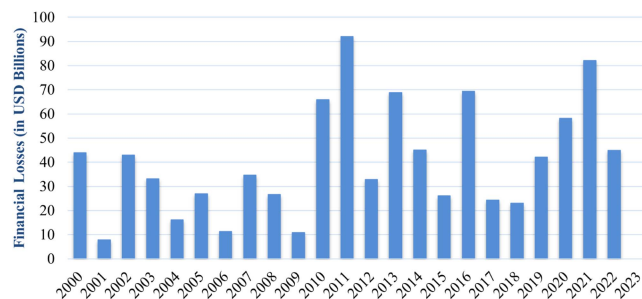Digital Object Identifier 10.1109/JSTARS.2024.3390579

Fig. 1. Annual flood-induced financial losses across continents. Source: EM-DAT: The Emergency Events Database; Université Catholique de Louvain (UCL) – CRED. Online. Available: http://www.emdat.be/.

financial losses ranged from $9 billion (USD) to $90 billion (USD), with an annual average of $10 billion (USD) (see Fig. 1). The 2022 and 2023 flooding events, including those that occurred in the United States and the United Kingdom, highlight the threat and damaging consequences of flooding. While countries around the world are exposed to flooding, the impacts are particularly disastrous to low- and middle-income (LMI) countries located in South and East Asia, Africa, and South America, which are also home to about 89% of the world's flood exposed population [1].

Although climate change is a major contributor of increased flood frequency [2], population growth and urbanization contribute to growing flood exposure and potential losses [1]. Due to the synergistic effect of population growth, expansion of infrastructures, lack of appropriate mitigation measures, and climate change, floods may impact billions of people and cause trillions of dollars in damage by 2100 [3], [4], [5]. In 2023, atmospheric rivers and tropical cyclone Hilary, both of which caused record-breaking rainfall, led to billions of dollars in economic loss in California, USA [6], [7]. The September 2023 flooding due to extreme rainfall caused the death of thousands of people in Libya and led to a humanitarian crisis [8]. These events not only underscore the unpredictability of flood hazards and subsequent losses, but also highlight the fact that despite access to resources, flood models, and early warning, developed countries such as the USA still grapple with the damaging consequences of flooding. It is, therefore, not surprising that flooding leads to catastrophic consequences in LMI countries that tend to lack access to models/tools, information, and resources to detect and respond in time to reduce impacts and enhance recovery.

Over the years, several open-source and proprietary global flood models have been developed to forecast flood events and their risk and severity as well as potential societal and financial impacts to assist communities with flood risk reduction. Proprietary models such as Fathom and KatRisk are used by the insurance industry to assess flood exposure and losses. Publicly available models such as Global Flood Risk (GLOFRIS), Catchment-based Macro-scale Floodplain (CAMA-UT), and European Centre for Medium-Range Weather Forecasts (ECMWF) are used by emergency managers, first responders, and other stakeholders to assess flood risks and predict flood events. Regardless of the use, these models generate products at different spatial resolutions over various geographies and return periods [9]. The variability in model implementation and their outputs inevitably makes them less accessible and usable among user communities, specifically first responders. Considering the consequences of flood hazards, an alternative solution is to have a global flood early warning system to inform and assist at-risk communities.

The Model of Models (MoM) contributes to this need. By deploying an ensemble approach to integrate hydrologic models and flood products derived from Earth observation (EO) data (i.e., optical and radar imagery), the model forecasts flood risk (probability of occurrence) globally every 24 h at a subwatershed level [10]. Based on the forecasted flood risk, early warnings along with potential exposure and impact information are disseminated to at-risk communities and stakeholders within high-risk subwatersheds using the Pacific Disaster Center's DisasterAWARE platform to undertake preparatory actions [11]. This ensemble framework combined with the alerting platform is a first step towards meeting the United Nation's initiative *Early Warnings for All* to reduce mortality and financial losses from natural disasters, especially, in LMI countries, such as Libya [12], [13].

The rest of this article is organized as follows. A discussion of global flood models is presented in Section II. Section III discusses the model and its implementation. The accuracy assessment approach and results are discussed in Section IV. Finally, Section V concludes this article.

II. GLOBAL FLOOD MODELS

Kar and Schuman [14] reviewed both publicly and privately available global flood models and tools with the general aim to assist stakeholders to better manage and respond to floods. The authors found that existing global flood models not only differ in their forecasting ability and mapping accuracy, but also in terms of methodology and applied physics, process representation, resolution, and frequency at which the outputs are updated. These models also use field data, remotely sensed observations, and hydrologic and hydrodynamic models (for more details, refer to EOTEC DevNet Flood Tracker [15]). Among more than 30 models identified in the flood tracker tool, the Global Flood Awareness System (GloFAS), managed by Copernicus, is probably one of the most widely used global flood forecasting models. It aims to facilitate response to flooding, particularly in countries that cannot forecast these events on their own [16]. Humanitarian

agencies, such as the United Nations' World Food Programme (UN WFP), also use this model along with other satellite-based mapping systems for emergency response [17]. Although these models and products are useful for emergency response, from an operational and user perspective, it is crucial to have a global flood early warning system to alert and provide situational awareness information with consistent accuracy and reliability to reduce flood risk and improve the resilience of LMI countries.

For emergency managers and first responders, it is critical to publicly access usable flood products in a timely manner. To achieve this goal, flood models should 1) be reliably available and accessible all the time, 2) generate interpretable and usable products, and 3) deploy an accepted methodology to produce consistent results across locations and events. The MoM meets these criteria by deploying an open-source framework that can incorporate any flood model and EO outputs to generate alerts and situational awareness products.

III. MODEL OF MODELS

The MoM has the following three components:
1) an ensemble model to delineate flood extent and forecast flood risk at 6-h and 24-h intervals;
2) calibration of flood risk based on EO data;
3) dissemination of alerts to impacted communities based on flood risk.
The following section discusses the steps and datasets used in each component to generate alerts.
1) GloFAS and Global Flood Monitoring system (GFMS), the two globally available hydrologic models for flood forecasting, are used to forecast flood risk in near real-time (daily and 6-h intervals). Given their variable spatial resolution outputs (discussed later), the flood risk is forecasted at the global subwatershed basin available from the World Resources Institute (WRI) [18]. The WRI dataset includes geometry information (subwatershed boundaries) for 3400 watershed basins across the world as well as the flood risk scores of each subwatershed basin based on historical riverine and coastal flooding events [Riverine Flood Risk (RFR) and Coastal Flood Risk (CFR)]. These scores, updated annually, represent riverine and coastal flooding impacts (i.e., populations at-risk, populations impacted by previous events, and existing flood protections). Forecasting flood risk at subwatershed basins allows emergency managers to assess impacted populations and infrastructures for resource planning as well as emergency response and preparedness activities.
2) GloFAS is flood forecasting and monitoring system that is independent of administrative and political boundaries [19]. The system couples weather forecasts with a hydrologic model to produce daily (24-h interval) flood forecasts and monthly seasonal streamflow outlooks to assist downstream countries with information on upstream river conditions. For MoM, the following attributes from GloFAS are used to derive a hazard score (HS): probability of a 2 year, 5 year, and 20 year flood occurrence, alert level (medium, high, severe) of the forecasted flood event, and

TABLE I
Weighting Scheme for Attributes Used to Derive HSs

Field	Description	Initial weighting	HS_Score
GFMS_TotalArea_km^2	Area of a flooded watershed in km^2 due to flood depth above the threshold	1pt for every 1 000km^2, max =10 (e.g., 8 900km^2 = 8.9)	HS_GFMS
GFMS_%Area	Percentage area of the flooded watershed - GFMSArea/WatershedArea	1pt for every 10%, Max = 10 (e.g., 66% = 10)	HS_GFMS
GFMS_MeanDepth(mm)	Mean Depth of flood within the watershed above threshold	1pt for every 10mm, max 10 (e.g., 56mm = 5.6)	HS_GFMS
GFMS_MaxDepth(mm)	Max Depth of flood within the watershed above threshold	1pt for every 10mm, max =10 (e.g., 89mm = 8.9)	HS_GFMS
GFMS_Duration	Number of 3-h intervals a specific area has been flooded (at least 100km^2 overlap in each interval)	Continuous days of at least 100km^2 overlap, 1 per day, Max= 10 (e.g., 66 h = 2.75)	HS_GFMS
GloFAS_20yr%	Probability that a flood of return period 20 year will be reached	10pt for 100\% Max = 10 (e.g., 66\% = 6.6)	HS_GloFAS
GloFAS_5yr%	Probability that a flood of return period 5 year will be reached	10pt for 100\% Max = 10 (e.g., 66\% = 6.6)	HS_GloFAS
GloFAS_2yr%	Probability that a flood of return period 2 year will be reached	10pt for 100\% Max = 10 (e.g., 66\% = 6.6)	HS_GloFAS
GloFAS_AlertLevel	Alert Level $1 - > 3$ with 3 greatest value	Level * 3.33, max 10 (e.g., 3 = 10)	HS_GloFAS
GloFAS_PeakForecasted	Number of days until peak forecast arrives at observation point	Weight in days where 1 =10, 2=9, … 10 or greater = 1	HS_GloFAS
HWRF_TotalArea_km^2	Area of the watershed impacted by the rainfall from HWRF	1pt for every 1 000km^2, max =10 (e.g., 8 900km^2 = 8.9)	HS_HWRF
HWRF_%Area	Percentage of the area of the watershed impacted by the rainfall from HWRF	1pt for every 5%, Max = 10 (e.g., 66% = 10)	HS_HWRF
HWRF_MeanRain (in inches)	Mean Rainfall within the watershed in inches	1pt for 2 in rain and add 1 pt for every 0.5 in rain increment, Max=10 (e.g.,4.5in =6)	HS_HWRF
HWRF_MaxRain (in inches)	Maximum Rainfall within the watershed in inches	1pt for 4 in rain and add 1pt for every 1 in rain increment, Max=10 (e.g., 4.5in =1.5)	HS_HWRF
DFO_1DayArea_km^2	Area of watershed in km^2 that is flooded based on one day observed data with cloud shadow masking applied	1pt for every 100 km^2, Max=10	HS_MODIS
DFO_1DayPercArea	Percentage area of the watershed that gets flooded based on one day observed data with cloud shadow masking applied	1pt for 1% area flooded, Max=10	HS_MODIS
DFO_2DayArea_km^2	Area of watershed in km^2 that is flooded based on two day observed data and cloud shadow masking is also applied	1.5pt for every 100 km^2, Max=15	HS_MODIS
DFO_2DayPercArea	Percentage area of the watershed that gets flooded based on two day observed data and cloud shadow masking is also applied	1.5pt for every 1% area, Max=15	HS_MODIS
DFO_3DayArea_km^2	Area of watershed in km^2 that is flooded based on three day observed data and cloud shadow masking is also applied	2.5pt for every 100 km^2, Max=25	HS_MODIS
DFO_3DayPercArea	Percentage area of the watershed that gets flooded based on three day observed data and cloud shadow masking is also applied	2.5pt for every 1% area, Max=25	HS_MODIS
VIIRS_1DayArea_km^2	Area of watershed in km^2 that is flooded based on one day observed data	1.5pt for every 100 km^2, Max=15	HS_VIIRS
VIIRS_1DayPercArea	Percentage area of the watershed that gets flooded based on one day observed data	1.5pt for 1% area flooded, Max=15	HS_VIIRS
VIIRS_5DayArea_km^2	Area of watershed in km^2 that is flooded based on five day composite observed data with cloud shadow masking applied	3.5pt for every 100 km^2, Max=35	HS_VIIRS
VIIRS_5DayPercArea	Percentage area of the watershed that gets flooded based on five day composite observed data with cloud shadow masking applied	3.5pt for every 1% area, Max=35	HS_VIIRS

Note:: HS GloFAS = HS derived from the summation of all GloFAS scores; HS GFMS = HS resulting from the summation of all GFMS scores; HS HWRF = HS derived from the summation of all HWRF scores; HS MODIS = HS derived from the summation of all MODIS scores (obtained from DFO); HS VIIRS = HS derived from the summation of all VIIRS scores.

peak forecast (# of days until the forecasted flood reaches the observed peak) (see Table I). Using the weighting scheme mentioned in Table I, each attribute is normalized to generate a score between 1 and 10. The weighted scores are subsequently summed together to derive HS for GloFAS (HS_GloFAS). The HS_GloFAS ranges from 0 to 50. Because GloFAS outputs are generated at specific locations, the estimated HS for all the locations existing within a subwatershed basin is averaged to compute the HS for the subwatershed HS$_{sw}$_GloFAS.

3) GFMS implements a hydrologic runoff and routing model to detect floods and their intensities using real-time precipitation data from the Tropical Rainfall Measuring Mission (TRMM) Multi-satellite Precipitation Analysis (TMPA) and Global Precipitation Measurement (GPM) Integrated Multi-Satellite Retrievals for GPM (IMERG) [20]. The model is functional between 50°N and 50°S latitudes and is implemented at 0.125° resolution. Using 13 years of retrospective model runs and surface water storage statistics (95th percentile plus parameters related to basin hydrologic characteristics), the model generates the following attributes every 3-h intervals: streamflow, surface water storage (depth in millimeters of surface water above dry ground), inundation variables at 1-km resolution, instantaneous precipitation and total precipitation based on past seven days, three days and the previous day, and forecasted flood risk 4–5 days into the future. For each subwatershed, spatial zonal statistics is used along with these attributes

to extract total area and percent area (in km^2) flooded, mean and maximum flood depth above threshold (in millimeters), and cumulative flood duration in hours if more than 100 km^2 of a subwatershed is flooded (see Table I). Each attribute is normalized between 1 and 10 as per the weighting scheme (see Table I). The weighted scores are summed together to compute HS for GFMS (HS_GFMS) that ranges between 0 and 50.

4) To compute flood risk (a probabilistic output), a Gaussian cumulative distribution function (cdf) is used to develop watershed level fragility functions. The cdf computes the probability of flood risk based on the forecasted HS for a subwatershed and its flood risk scores (RFR and CFR). In MoM, the function uses log of the HS, log of the flood risk score (as mean), and 1 unit as standard deviation (assumes normal distribution).

Although GFMS outputs are available at every 3-h intervals, MoM forecasted outputs are generated at every 6-h intervals to match the time intervals at which Hurricane Weather Research and Forecasting (HWRF) model outputs are updated. First, every 6 h, the maximum HS_GFMS over a 6-h duration is combined with the (HS$_{sw}$_GloFAS) to generate forecasted flood risk at subwatershed level (HS_Base = HS_GFMS + HS$_{sw}$_GloFAS).

If either GloFAS or GFMS fails to forecast a flood event, the HS of the model with forecasted outputs is weighted twice to compute flood risk. For instance, if HS$_{sw}$_GloFAS = 0, HS_Base = 2 * HS_GFMS. This ensures the total HS_Base score ranges between 0 and 100 across all the subwatersheds. Second, the WRI flood risk scores for subwatersheds (RFR and CFR) are rescaled from 0–5 to 0–100 to match the HS range (0–100). These values provide the median of the cdf fragility function based on risk scores. Third, these risk scores and HS_Base are used in a cdf to compute flood risk (FR_Base) and identify the subwatersheds at high risk of flooding.

5) Neither GloFAS nor GFMS incorporates the rapidly changing flood hazard conditions during a landfalling tropical storm. To incorporate risks associated with tropical storms, the HWRF model outputs that are updated every 6-h with forecasted advisory are used [21] to determine the total and percent area of a subwatershed receiving rainfall, and the minimum, maximum, and total rainfalls received by a subwatershed. These attributes are normalized (0–10) using the weighting scheme (see Table I) and summed together to compute a HS for tropical storms (HS_HWRF). The HS_HWRF is compared with HS_Base, and the subwatersheds with maximum HS (HS_HWRF > HS_Base) are flagged for coastal flooding (Flag = 1) and assigned an HS HS1 (maximum between HS_HWRF and HS_Base). For these subwatersheds, the flood risk (FR1) is recomputed using cdf with HS1, RFR, and CFR.

6) To calibrate MoM outputs, flood products from the Moderate Resolution Imaging Spectroradiometer (MODIS)

satellite and the Visible Infrared Imaging Radiometer Suite (VIIRS) instrument are used. The MODIS Water Product (MWP) provides daily MODIS Surface Water (MSW) and MODIS Flood Water (MFW) maps, which are acquired from the Dartmouth Flood Observatory at approximately 250-m resolution [22]. The georectified and cloud cover corrected 1-day, 2-day, and 3-day MWP composites are used to compute the percent and total area flooded at the subwatershed level. Each attribute is normalized using the weighting scheme in Table I, which are then combined together to compute an HS (HS_MODIS). HS_MODIS is compared with HS1 (HS_MODIS > HS1) and the subwatersheds with maximum HS are flagged (*Flag=2*) and assigned HS2. The flood risk (FR2) for these subwatersheds is recalculated using cdf with HS2, RFR, and CFR scores. HS2 represents HSs for those subwatersheds that are experiencing maximum flooding as per the forecasted models (GloFAS, GFMS, and HWRF) and EO data from MODIS.

7) The VIIRS 1-day and 5-day composite flood products are available at 375-m resolution. Each 375-m pixel is categorized into cloud, snow cover, river/lake ice cover, shadows, clear-sky land, normal open water, suprasnow/ice water or mixed ice and water, and flooding water fractions. A pixel with more than 40% area covered with flood water is considered a flooded pixel [23]. Because flooded pixels represent surface water extent across different land uses, the world population data, available at 100-m resolution from WorldPop [24], are used to mask out wetlands and unpopulated areas. For each subwatershed, the total and percent area flooded are computed using the masked 1-day and 5-day composite surface water extent layer. These attributes are then normalized using the weighting scheme (see Table I) and combined to compute an HS (HS_VIIRS). HS_VIIRS is compared with HS2 (HS_VIIRS > HS2); the subwatersheds identified to be flooding by VIIRS are flagged (*Flag=3*) and assigned the maximum HS (HS3), which is used along with RFR and CFR to recompute flood risk (FR3).

8) The final flood risk score (FR3) is used to determine alerting categories *Information* (0% < FR3 < 35%), *Advisory* (35% $\leqslant$ FR3 < 60%), *Watch* (60% $\leqslant$ FR3 < 80%), and *Warning* (FR3 > 80%) and trigger alert dissemination using the DisasterAWARE multihazard alerting platform. The alerting categories were empirically determined based on MoM performance during 2020–2022 along with observed flood events during the same time. Alerts are disseminated for inland subwatersheds provided they were flagged for active flooding according to MODIS and VIIRS (Flag = 2 and Flag = 3) and have a high base flood risk (FR3 > 60%). In case of coastal subwatersheds, alerts are disseminated provided the subwatersheds have been flagged for coastal flooding (Flag = 1 and Flag = 2 and Flag = 3) and have a high base flood risk (FR3 > 60%) Fig. 2).
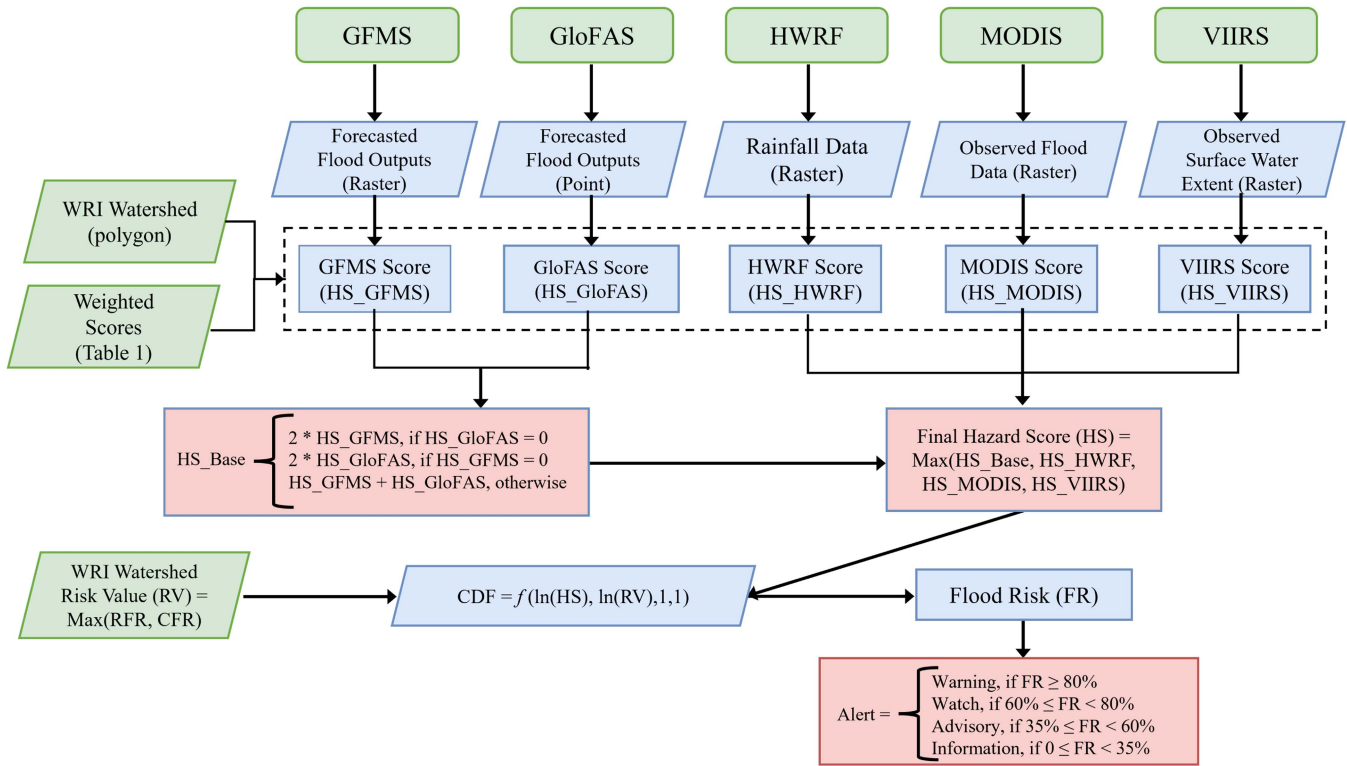
Fig. 2. Conceptual implementation of MoM.

TABLE II
SELECTED FLOOD EVENTS FOR MoM PERFORMANCE ASSESSMENT AND REFERENCE SOURCES (Y = THE EVENT WAS DETECTED—N = THE EVENT WAS NOT DETECTED)

Region	Country	Flood type	Year	Start date	End date	MoM	EM-DAT	GFM social media	Copernicus GFM	International Charter
South Asia	Pakistan	Monsoon flood	2022	mid-June	November	Y	Y	Y	Y	Y
Africa	Sierra Leone	Flash flood	2022	28-August	September	Y	Y	Y	Y	N
Africa	Chad	Fluvial flood	2022	July	October	Y	Y	Y	Y	Y
Europe	Italy	Flash flood	2022	15-September	16-September	Y	N	Y	N	N
South America	Brazil	Pluvial flood	2022	28-November	2-December	Y	Y	N	Y	N
Australia	Australia	Pluvial–fluvial flood	2022	22-February	April	Y	Y	Y	Y	N
North America	United States	Atmospheric River	2023	9-January	10-January	Y	Y	Y	Y	N
South Asia	Bangladesh	Monsoon flood	2022	May	September	Y	Y	Y	Y	Y
Southeast Asia	Philippines	Tropical storm	2022	28-October	31-October	Y	Y	Y	Y	Y
Flood type description: pluvial flood: flood caused by excess rainfall; fluvial flood: river flooding; flash flood: intense flooding of short duration; atmospheric river: long and narrow atmospheric streams of water vapor holding extremely large quantities of water that can be released as rain when making landfall										

IV. MoM VALIDATION AND ACCURACY ASSESSMENT

Assessing the performance of MoM from a user perspective is crucial to ensure its effectiveness in disseminating alerts for flood events to the correct location(s). While scientific accuracy is important, user satisfaction relies on timely, precise notifications that align with their expectations. User-centric evaluation considers factors such as the model's ability to issue alerts based on actual event location and how many times the model alerted correctly, preferably for all types of flood events. By prioritizing user-centric metrics, the reliability and trustworthiness of flood alerts can be enhanced, thereby ultimately improving public safety and response during critical events.

To assess the accuracy and reliability of MoM, the model outputs were compared with nine events of various sizes and severity (see Table II) that occurred in different continents and caused significant losses. Specifically, the assessment focused on MoMs reliability in identifying a flood event and its spatial extent (subwatersheds) for alert dissemination in comparison to other global models.

The selected flood events guarantee global coverage, diversity in event types (e.g., flash floods, tropical storms, and atmospheric rivers), and high severity based on impacted population according to the media and humanitarian agency reports. For comparison, a list of flood events was retrieved from the EM-DAT database, the Global Flood Monitor based on social media [25], and the International Charter for Space and Major Disasters (referred as Int. Charter). An event was considered identified if it was recorded in the EM-DAT or social media database for the timeframes and geographic locations according

TABLE III
MoM Spatial Accuracy Assessment and GFMS Performance Assessment Results Using Copernicus GFM Data for the Selected Events

Event	MoM Watch/ Warning			MoM with Advisory			MoM all levels			GFMS		
	Detect	No.	%	Detect	No.	%	Detect	No.	%	Detect	No.	%
Pakistan	FALSE	38	39%	FALSE	24	24%	FALSE	3	3%	FALSE	30	31%
	TRUE	60	61%	TRUE	74	76%	TRUE	95	97%	TRUE	68	69%
	Total	98	100%	Total	98	100%	Total	98	100%	Total	98	100%
Sierra Leone	FALSE	5	42%	FALSE	2	17%	FALSE	0	0%	FALSE	3	25%
	TRUE	7	58%	TRUE	10	83%	TRUE	12	100%	TRUE	9	75%
	Total	12	100%	Total	12	100%	Total	12	100%	Total	12	100%
Chad	FALSE	9	11%	FALSE	2	3%	FALSE	0	0%	FALSE	0	0%
	TRUE	71	89%	TRUE	78	98%	TRUE	80	100%	TRUE	80	100%
	Total	80	100%	Total	80	100%	Total	80	100%	Total	80	100%
Brazil	FALSE	5	83%	FALSE	3	50%	FALSE	0	0%	FALSE	3	50%
	TRUE	1	17%	TRUE	3	50%	TRUE	6	100%	TRUE	3	50%
	Total	6	100%	Total	6	100%	Total	6	100%	Total	6	100%
Australia	FALSE	56	86%	FALSE	42	65%	FALSE	0	0%	FALSE	37	57%
	TRUE	9	14%	TRUE	23	35%	TRUE	65	100%	TRUE	28	43%
	Total	65	100%	Total	65	100%	Total	65	100%	Total	65	100%
United States	FALSE	17	85%	FALSE	10	50%	FALSE	0	0%	FALSE	9	45%
	TRUE	3	15%	TRUE	10	50%	TRUE	20	100%	TRUE	11	55%
	Total	20	100%	Total	20	100%	Total	20	100%	Total	20	100%
Bangladesh	FALSE	10	28%	FALSE	4	11%	FALSE	0	0%	FALSE	17	47%
	TRUE	26	72%	TRUE	32	89%	TRUE	36	100%	TRUE	19	53%
	Total	36	100%	Total	36	100%	Total	36	100%	Total	36	100%
Philippines	FALSE	4	57%	FALSE	1	14%	FALSE	0	0%	FALSE	1	14%
	TRUE	3	43%	TRUE	6	86%	TRUE	7	100%	TRUE	6	86%
	Total	7	100%	Total	7	100%	Total	7	100%	Total	7	100%

No. indicates the number of instances (combinations of catchments and dates) where MoM or GFMS identified (TRUE) or did not identify (FALSE) flooding.
Note:: The flooding in the Marche Region of Italy in 2022 was not included in this part of the analysis because no satellite imagery was readily available for flood impacted areas.

to the reports. In case of MoM, an event was considered detected if a "Warning" or "Watch" was disseminated to any of the subwatersheds within the event's geographic location.

The spatial accuracy of MoM outputs was assessed by comparing the high flood risk subwatersheds with Copernicus Global Flood Monitoring system (Copernicus GFM) imagery for the selected timeframes and geographic locations. Copernicus GFM was used for comparison because it is independent from MoM and uses the Sentinel-1 synthetic aperture radar (SAR) images. Spatially, if an imagery contained flooded areas for an event that aligned geographically with the subwatersheds identified to be of high risk by MoM, then the flooded subwatersheds were considered to be accurate. For long-duration events with significant geographic coverage, flood maps and imagery from Copernicus GFM were searched and obtained for a random set of dates. Upon geo-registering the maps and imagery, the maps and imagery where flooding was detected were compared with the subwatersheds based on the alerting category (Warning, Watch, Advisory, and Information). Because MoM outputs are generated every 6 h, for simplicity, the highest alert level recorded for a subwatershed within 24 h was used for comparison. In addition, the overall event statistics was also computed that included all the subwatersheds identified to be flooding by MoM by calculating the percentage of times MoM alerts (all categories)

were generated for a subwatershed where Copernicus GFM also detected a flooding event.

The performance of MoM was also evaluated by comparing its outputs for the selected events with the performance of a single model (GFMS) to show the benefits of having an ensemble approach to flood forecasting and alerting. This approach is similar to ablation study used in machine learning to examine the contribution of a component to an overall system and assess its sensitivity. The flooded subwatersheds identified by the imagery collected from Copernicus by date were compared with GFMS and MoM outputs. Although both MoM and GFMS generate outputs every 6 and 3 h, respectively, a single output value per day by subwatershed based on the highest alert level according to MoM and the highest area flooded in a subwatershed according to GFMS were used. It was assumed that GFMS forecasted flooding when the area of a flooded subwatershed was higher than zero. Because GloFAS outputs are generated at specific locations within a subwatershed, it was not feasible to compare GloFAS outputs with MoM.

V. RESULTS AND DISCUSSION

Despite the diversity in flood events, results (see Table III) indicate that MoM was successful in identifying the flood events
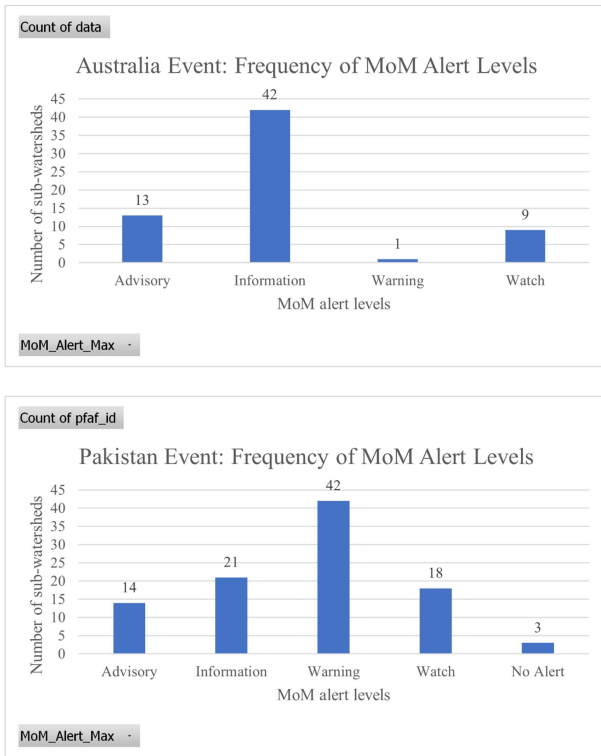
Fig. 3. Frequency distribution of the subwatersheds identified by MoM in each alert category during (a) 2022 Australia flood and (b) 2022 Pakistan flood. The subwatersheds that were missed by MoM are represented as "no alert" category.

while other global models and systems missed at least one or more events. For instance, the September 2022 Italy flash flood in the Marche Region was missed by most systems including Copernicus GFM, which did not have any images of the flooded areas, probably due to its short duration. This flood event, however, was captured by MoM for alerting purposes.

Overall, MoM performed well for most events (see Table III) regardless of the alert categories. It is significant to note that MoM reliably generated early warning for 100% of the flooded subwatersheds in seven events. For high severity floods (Chad and Pakistan flooding, 2022), 61% and 89% of the flooded subwatersheds were identified to be in Watch and Warning categories in Pakistan and Chad, respectively, which were also detected by the Copernicus GFM system. Based on the frequency distribution of MoM alert levels for the Pakistan and Australian floods (see Figs. 2 and 3), it is evident that the Australian flood, a result of pluvial–fluvial flooding, also predominantly received "Information" while the Pakistan flooding received frequent "Warnings."

Following the 2023 Libyan flooding, the World Meteorological Organization emphasized the need for early warning to assist countries lacking technologies and human resources to reduce extreme weather impacts on society [13]. MoMs current capability to trigger alerts ahead of time fills this gap. However, for emergency management, all alert levels should be considered rather than just the "Warning" and "Watch" categories because an "Advisory" still generates alerts, albeit for an area with a lower probability of flood occurrence. A low-probability event

TABLE IV
MoM PRODUCTS AND THEIR FORMATS

Output	Short Description	Data type	Format
Impacted subbasins	Subbasins with forecasted flood risk	Geospatial (Subbasin and administrative boundaries)	GeoJson
Alerting level	Alerting level for subbasins based on flood risk. Categories included: Warning, Watch, Advisory and Information.	Alert categories for subbasins	CSV
Important subbasin attributes	Attributes of input datasets, weighted scores, HSs for each input model/EO dataset, forecasted and calibrated flood risk scores	Attribute table for subbasins	CSV

can have high severity impacts, depending upon communities and infrastructures exposed, mitigation strategies in place, and resource availability. For instance, during the 2022 Australian flood, most of the flooded subwatersheds were categorized to be low-risk (alert category "Information") by MoM (see Fig. 3), but it was considered as one of the worst floods [26]. Furthermore, an advisory alert can change to Watch or Warning in subsequent forecasting days depending upon the event. Therefore, it is paramount for decision makers in LMI countries to have access to alerting information to undertake emergency management efforts to reduce losses.

In terms of spatial performance, the consistency between MoM and observed flooded areas from SAR is relatively low for rapid onset events (e.g., atmospheric river induced flooding or pluvial floods in Brazil) or events that are covering extremely large areas spreading across many hydrological basins, such as the Australia flood. Of course, for these types of events, satellite remote sensing has significant limitations, particularly, the inability to precisely capture rapid onset events due to infrequent orbital revisits and to accurately map floods in vegetated and built-up areas. From this perspective, MoM is well positioned to not only detect flood events that may or may not be captured by satellite/sensors, but also to monitor the status of a flood event over a period of time.

Between GFM and MoM (see Table III), if we consider all alert levels, it is clear that MoM performed better in all events except for in Chad, where both models excelled. Considering MoM alert levels (i.e., Warning, Watch, and Advisory), MoM performed better than or equal to GFM for high-probability flood events. These results show the advantage of having a MoM approach that leverages other models to identify events even when one or more models fail to forecast or detect flooding.

VI. CONCLUSION AND FUTURE WORK

The current deployment of MoM produces the following three main products: 1) impacted subwatershed layer, 2) alerting level, and 3) subwatershed attributes every 6 h that are useful for emergency management, downstream analytics (such as social and infrastructure impact assessment), and alerting (see Table IV). The integration of MoM into the DisasterAWARE platform (refer to the work in [27] for more information) as
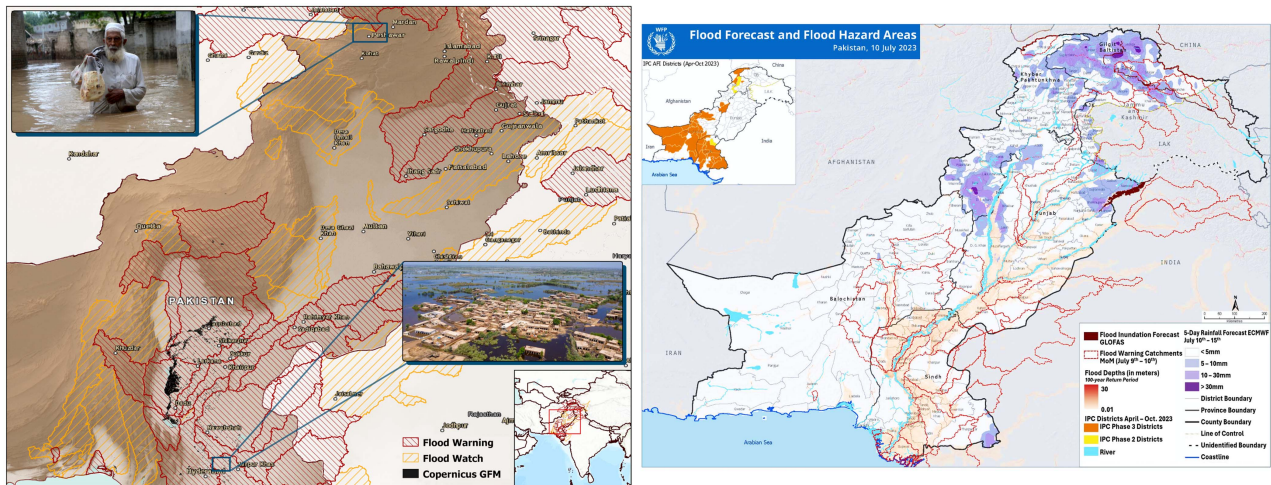
Fig. 4. Pakistan floods as captured by MoM in 2022 (a) and 2023 (b). Note the map shown in (b) is a UN WFP Country Office map, showing the MoM alerting regions integrated in the Country Office GIS analysis.

well as these data products allows early flood warning and generation of flood impact scenarios for emergency management activities. The ensemble approach using forecasted and observed flood products also 1) eliminates the challenge of interpreting outputs from multiple flood models that can be confusing for stakeholders, 2) provides the opportunity to identify high flood risk areas using the longitudinal data for resource planning, and 3) enables monitoring and detection of different flood types (pluvial, fluvial, and tropical cyclone) more reliably (see Fig. 4).

The current version of MoM has two limitations. First, the model does not capture flash floods, flooded areas with smaller footprints, and flooding resulting from rapid onset glacial and snow melt. Second, the flood probability is determined at sub-watershed levels that may include several communities with different flood risks. While the fragility approach used in MoM amplifies flood risk that could be useful for emergency managers in LMI countries to prepare for future flood events, this can be expensive as it identifies all communities within a subwatershed to have the same risk, which may not be the case. From an emergency management perspective, the cost of resource planning needed for a low-risk community with little social and infrastructure exposure would be less than that of a high-risk community with high exposure. Because the current implementation does not distinguish the risk level across communities, the use of model outputs can be expensive for certain communities. Future enhancements of MoM, therefore, will focus on the following:

1) calibrating model weights and inputs based on observed model performance;
2) deploying a machine learning algorithm to automatically adjust weights and parameters to improve reliability and autoclassify flood risk for alerting purposes;
3) downscaling estimated flood risk to community level by incorporating localized flood forecasting model outputs.

For precise determination of flood extent and impact areas, the next generation MoM will incorporate SAR and digital elevation model datasets to compute flood depth at a finer resolution, which is dependent on SAR availability. Regional flood models will also be integrated into MoM to increase the precision of

flood outputs. The flood extent and depth information will be used to refine exposure and impact assessment outputs, which will further increase the usefulness of MoM for the emergency management community and assist them with geo-targeted response efforts. Despite their near real-time availability, MODIS and VIIRS outputs suffer from cloud cover. To overcome this issue, the future version of MoM will also incorporate other optical sensors, such as those onboard the NOAA 20 and NOAA 21 satellites, as well as precipitation data. Beyond DisasterAWARE, the MoM outputs will be disseminated via cloud deployment to different stakeholders, such as the WFP country offices, to generate agency-specific analytical outputs.

REFERENCES

[1] J. Rentschler, M. Salhab, and B. A. Jafino, "Flood exposure and poverty in 188 countries," *Nature Commun.*, vol. 13, no. 1, Jun. 2022, Art. no. 3527. [Online]. Available: https://www.nature.com/articles/s41467-022-30727-4

[2] Intergovernmental Panel On Climate Change, *Climate Change 2021—The Physical Science Basis: Working Group I Contribution to the Sixth Assessment Report of the Intergovernmental Panel on Climate Change*, 1st ed. Cambridge, U.K.: Cambridge Univ. Press, Jul. 2023. [Online]. Available: https://www.cambridge.org/core/product/identifier/9781009157896/type/book

[3] E. Kirezci et al., "Projections of global-scale extreme sea levels and resulting episodic coastal flooding over the 21st century," *Sci. Rep.*, vol. 10, no. 1, Jul. 2020, Art. no. 11629. [Online]. Available: https://www.nature.com/articles/s41598-020-67736-6

[4] R. J. Nicholls et al., "Author correction: A global analysis of subsidence, relative sea-level change and coastal flood exposure," *Nature Climate Change*, vol. 11, no. 7, pp. 634–634, Jul. 2021. [Online]. Available: https://www.nature.com/articles/s41558-021-01064-z

[5] H. C. Winsemius et al., "Global drivers of future river flood risk," *Nature Climate Change*, vol. 6, no. 4, pp. 381–385, Apr. 2016. [Online]. Available: https://www.nature.com/articles/nclimate2893

[6] Moody's RMS Estimates US5-7 Billion in Total U.S. Economic Losses from California Flooding Moody's RMS, Jan. 2023. [Online]. Available: https://www.rms.com/newsroom/press-releases/press-detail/2023-01-25/moodys-rms-estimates-us5-7-billion-in-total-us-economic-losses-from-california-flooding

[7] Hurricane Costs, 2023. [Online]. Available: https://coast.noaa.gov/states/fast-facts/hurricane-costs.html

[8] Libya: Humanitarian Response Ramps Up as Floods of 'Epic Proportions' Leave Thousands Dead UN News, 2023. [Online]. Available: https://news.un.org/en/story/2023/09/1140652

[9] J. P. M. Aerts, S. Uhlemann-Elmer, D. Eilander, and P. J. Ward, "Comparison of estimates of global flood models for flood hazard and exposed gross domestic product: A China case study," *Natural Hazards Earth Syst. Sci.*, vol. 20, no. 12, pp. 3245–3260, 2020. [Online]. Available: https://nhess.copernicus.org/articles/20/3245/2020/

[10] G. J.-P. Schumann, B. Kar, P. Sharma, D. Bausch, J. Wang, and M. Glasscoe, "Early warning for all with a model of models approach," in *Proc. IEEE Int. Geosci. Remote Sens. Symp.*, 2023, pp. 456–459.

[11] P. Sharma et al., "DisasterAWARE—A global flood alerting platform for flood events," in *Proc. ISPRS Ann. Photogrammetry Remote Sens. Spatial Inf. Sci., 13th GeoInformation Disaster Manage. Conf.*, 2020, pp. 107–113.

[12] G. Schumann, "Pioneering universal early warning systems for natural disasters," 2022. [Online]. Available: https://www.innovationnewsnetwork.com/the-need-for-early-warning-systems-that-can-cover-everyone/27864/

[13] "Libya floods show need for multi-hazard early warnings, unified response world meteorological organization," 2023. [Online]. Available: https://wmo.int/media/news/libya-floods-show-need-multi-hazard-early-warnings-unified-response#:~:text=%22The%20tragedy%20in%20Libya%20highlights,Petteri%20Taalas

[14] B. Kar and G. Schumann, "Reproducibility and replicability of flood models," *Hydrol. Processes*, vol. 36, no. 9, 2022, Art. no. e14666. [Online]. Available: https://onlinelibrary.wiley.com/doi/abs/10.1002/hyp.14666

[15] "Flood tools," 2023. [Online]. Available: https://eotec-dev.ceos.org/tools/

[16] L. Alfieri et al., "GloFAS – global ensemble streamflow forecasting and flood early warning," *Hydrol. Earth Syst. Sci.*, vol. 17, no. 3, pp. 1161–1175, 2013. [Online]. Available: https://hess.copernicus.org/articles/17/1161/2013/

[17] R. E. Emerton et al., "Continental and global scale flood forecasting systems," *WIREs Water*, vol. 3, no. 3, pp. 391–418, May 2016. [Online]. Available: https://onlinelibrary.wiley.com/doi/10.1002/wat2.1137

[18] Watersheds of the World, 2020. [Online]. Available: https://www.wri.org/watersheds-world

[19] Global Flood Awareness System, 2023. [Online]. Available: https://www.globalfloods.eu/general-information/about-glofas/

[20] Global Flood Monitoring, 2023. [Online]. Available: http://flood.umd.edu/

[21] V. Tallapragada et al., "Hurricane Weather Research and Forecasting (HWRF) model: 2014 scientific documentation," 2022. [Online]. Available: https://www.aoml.noaa.gov/ftp/hrd/annane/osse/upgrade_to_operational/HWRFv3.6a_ScientificDoc.pdf

[22] MODIS NRT Global Flood Product Earthdata, 2023. [Online]. Available: https://www.earthdata.nasa.gov/learn/find-data/near-real-time/modis-nrt-global-flood-product

[23] NOAA VIIRS/ABI Flood Products, 2019. [Online]. Available: https://www.ssec.wisc.edu/flood-map-demo/wp-content/uploads/sites/38/2019/06/ABI_VIIRS-Flood-mapping-overview-document_042219_compressed.pdf

[24] Open Access to Global Development Data - WorldPop, 2023. [Online]. Available: https://www.worldpop.org/datacatalog/

[25] J. A. De Bruijn, H. De Moel, B. Jongman, M. C. De Ruiter, J. Wagemaker, and J. C. J. H. Aerts, "A global database of historic and real-time flood events based on social media," *Sci. Data*, vol. 6, no. 1, Dec. 2019, Art. no. 311. [Online]. Available: https://www.nature.com/articles/s41597-019-0326-9

[26] 2022 Australian Flooding - Center for Disaster Philanthropy. 2022. [Online]. Available: https://disasterphilanthropy.org/disasters/2022-australian-flooding/

[27] B. Kar et al., "Integrated model of models for global flood alerting," in *WIT Trans. on the Built Environ.*. Southampton, U.K.: WIT Press, Dec. 2020, pp. 73–83. [Online]. Available: http://library.witpress.com/viewpaper.asp?pcode=FRIAR20-007-1

Bandana Kar received the Ph.D. degree in geography (geoinformatics and modeling flood impacts) from the University of South Carolina, Columbia, SC, USA, in 2008.

She was a Senior Scientist with Oak Ridge National Laboratory from 2017 to 2022 and a tenured Associate Professor with the University of Southern Mississippi from 2008 to 2017. She is currently an AAAS Science, Technology, and Policy Fellow for building decarbonization with the U.S. Department of Energy. Her research in energy and urban resilience has been funded by NASA, NSF, DHS, and DOE.

Guy J.-P. Schumann received the Ph.D. degree in geography (modeling and remote sensing of floods) from the University of Dundee, Dundee, U.K., in 2008.

He is currently a Senior Scientist working on disaster and water risk projects. He currently holds affiliations in the USA and Europe and is a Visiting Fellow with the University of Bristol. He is also an Expert Consultant for WFP and FAO of the UN. He was a Lecturer with the University of Bristol, U.K., from 2008 to 2012 and worked with NASA JPL from 2012 to 2014.

Marina T. Mendoza received the Ph.D. degree in urban planning from the University of Buenos Aires, Buenos Aires, Argentina, in 2019.

She is currently working on disaster risk management and climate change adaptation with government agencies and commercial clients. She has more than 10 years of experience in disaster risk management of floods, earthquakes, and wildfires.

Dr. Mendoza is a recipient of a scholarship from the Politecnico di Milano, Italy, for the Ph.D. degree.

Doug Bausch received the M.S. degree in geology from Northern Arizona University, Flagstaff, AZ, USA, in 1989.

He is currently the Director of Data Science with Niyam IT, Leesburg, VA, USA, primarily supporting the development and implementation of state-of-the-art natural hazard loss and risk assessment tools. He has more than 25 years of experience assisting states and communities, across the USA and abroad, in developing sound risk and vulnerability assessments to support all-hazard response, mitigation, recovery, and preparedness planning.

Jun Wang received the M.S. degree in geomorphology from Peking University, Beijing, China, in 1999.

He is currently a GIS Specialist with Cyberinfrastructure Integration Research Center (CIRC), Indiana University, Bloomington, IN, USA. He has been involved in NASA-funded projects on natural disasters for more than a decade. His research interests include large-scale spatial data processing, web-application, and visualization using Cloud computing technology.

Margaret T. Glasscoe received the Ph.D. degree in geology from the University of California Davis, Davis, CA, USA, in 2015.

She is currently a Researcher with the University of Alabama, Huntsville, AL, USA. She was a Contractor with the Marshall Space Flight Center and a Research Scientist with NASA Jet Propulsion Laboratory for 17 years and worked with the NASA Disasters Program as a Coordinator for eight years. Her research interest includes the development of flood- and earthquake-focused decision support systems and products.

Prativa Sharma received the Ph.D. degree in civil engineering from the University of Missouri Kansas City, Kansas City, MO, USA, in 2021, focused on resilience assessment of the civil infrastructure against natural hazards.

She is currently a Design Engineer with Bennett & Pless, Atlanta, GA, USA. During her doctoral study, she worked on the model of model deployment as part of the NASA funded project "Advancing access to global flood modeling and alerting using the PDC disaster AWARE platform and remote sensing technologies."